

A Novel MIMO SMC for Comprehensive Unified Control of the Cascaded DC-DC and DC-AC Converters in Grid Connected Photovoltaic Systems

Mansour hosseini firouz¹, Fereshteh Radmand¹, Mahdi Salimi², and Ebrahim Babaei³

¹Islamic Azad University Ardabil Branch

²University of Greenwich Faculty of Engineering and Science

³University of Tabriz Faculty of Electrical and Computer Engineering

February 22, 2024

Abstract

It is well-known that DC-DC boost converters are cascaded with DC-AC inverters for grid connection of the photovoltaic (PV) systems. In the traditional control approaches, the mentioned DC-DC and DC-AC converters are controlled separately to facilitate the controller design problem. However, from the controller design viewpoint, the overall structure of the grid connected PV generator is a multi-input multi-output (MIMO) system. The duty-cycle of the DC-DC converter and Inverter modulation index are the control inputs and on the other hand, generated photovoltaic DC power, and exported power to the grid are control outputs. Moreover, the inverter DC link voltage should be stabilized by the closed-loop controller as well as an internal control output. If controllers are designed separately, it means that the interaction between DC-DC and DC-AC controllers isn't considered accurately and since the isolated models of DC-DC converter and DC-AC inverter are extracted based on some approximated assumptions, separate controller design cannot guarantee stability and robustness of the whole system in a wide range of operation. To cope with these problems, in this paper, a novel MIMO sliding mode controller (SMC) is developed for comprehensive closed-loop control of the DC-DC boost converter cascaded with a single-phase DC-AC grid connected photovoltaic inverter. In the proposed approach, the dynamic model of whole system is developed comprehensively at first and then a unique MIMO controller is designed to control both DC-to-AC and DC-to-DC converters together. To cope with the nonlinear characteristic of the system and uncertainty of model parameters in a wide range, a fixed-frequency SMC is developed using the comprehensive state space model of the closed loop system. In the proposed MIMO-SMC controller, the AC power (which is exported to the grid) and operating point of the PV source are controlled via inverter modulation index and duty cycle of the DC-DC boost converter respectively. Another major advantage of the proposed system is mitigating the non-minimum phase characteristic of the boost converter through the indirect control of inverter DC link capacitor. To evaluate the performance of the designed control system, simulation results are compared with a standard linear PI controller. It is shown that the developed system has zero steady-state error and enjoys faster dynamic response during the start-up and step changes of AC and DC current references. Moreover, it can maintain the stability of closed-loop systems in a wide range of operations.

A Novel MIMO SMC for Comprehensive Unified Control of the Cascaded DC-DC and DC-AC Converters in Grid Connected Photovoltaic Systems

Fereshteh Radmand

Department of Electrical Engineering, Ardabil Branch, Islamic Azad University, Ardabil, Iran
f.radmand@iauardabil.ac.ir

Mansour Hosseini Firouz (corresponding author)

Department of Electrical Engineering, Ardabil Branch, Islamic Azad University, Ardabil, Iran
hosseini.firooz@iauardabil.ac.ir

Mahdi Salimi

Faculty of Engineering and Science, University of Greenwich, Medway, Kent, ME4 4TB, UK
m.salimi@greenwich.ac.uk

Ebrahim Babaei

Faculty of Electrical and computer Engineering, University of Tabriz, Tabriz, Iran
e-babaei@tabrizu.ac.ir

Abstract :It is well-known that DC-DC boost converters are cascaded with DC-AC inverters for grid connection of the photovoltaic (PV) systems. In the traditional control approaches, the mentioned DC-DC and DC-AC converters are controlled separately to facilitate the controller design problem. However, from the controller design viewpoint, the overall structure of the grid connected PV generator is a multi-input multi-output (MIMO) system. The duty-cycle of the DC-DC converter and Inverter modulation index are the control inputs and on the other hand, generated photovoltaic DC power, and exported power to the grid are control outputs. Moreover, the inverter DC link voltage should be stabilized by the closed-loop controller as well as an internal control output .If controllers are designed separately, it means that the interaction between DC-

DC and DC-AC controllers isn't considered accurately and since the isolated models of DC-DC converter and DC-AC inverter are extracted based on some approximated assumptions, separate controller design cannot guarantee stability and robustness of the whole system in a wide range of operation. To cope with these problems, in this paper, a novel MIMO sliding mode controller (SMC) is developed for comprehensive closed-loop control of the DC-DC boost converter cascaded with a single-phase DC-AC grid connected photovoltaic inverter. In the proposed approach, the dynamic model of whole system is developed comprehensively at first and then a unique MIMO controller is designed to control both DC-to-AC and DC-to-DC converters together. To cope with the nonlinear characteristic of the system and uncertainty of model parameters in a wide range, a fixed-frequency SMC is developed using the comprehensive state space model of the closed loop system. In the proposed MIMO-SMC controller, the AC power (which is exported to the grid) and operating point of the PV source are controlled via inverter modulation index and duty cycle of the DC-DC boost converter respectively. Another major advantage of the proposed system is mitigating the non-minimum phase characteristic of the boost converter through the indirect control of inverter DC link capacitor. To evaluate the performance of the designed control system, simulation results are compared with a standard linear PI controller. It is shown that the developed system has zero steady-state error and enjoys faster dynamic response during the start-up and step changes of AC and DC current references. Moreover, it can maintain the stability of closed-loop systems in a wide range of operations.

Keywords: non-minimum phase, DC-DC boost converter, multi-input multi-output, cascaded converters, grid-connected inverter averaged state space model

1- Introduction

Despite the recent investments on the traditional electric power plants, power systems are still struggling to respond to the increasing energy demand. Considering the environmental problems and very high cost of fossil-based energy resources, replacing the traditional energy resources with renewable generators is a promising idea [1] and for this reason, application of photovoltaic (PV) and wind energies have been increased sharply in recent years [2]. Based on the long-term planning, photovoltaic systems will be assumed as a reliable candidate for electricity energy supply [3]. The application of solar energy for electricity generation is very beneficial from the environmental perspective as well. Moreover, since distributed generators (DG) e.g. PV system can be utilized next to load centres and within the distribution networks, overall efficiency of the electric grid can be improved if penetration rate of DGs increases significantly. So, it isn't a surprising news that about 125 GW of the photovoltaic system will be installed worldwide between 2020 and 2024 [4]. Compared to 2018, it is expected that the electricity generation using PV systems will be approximately increased by six times at the end of 2050 and as a result, the total application of PV systems will be more than 372GW by the end of 2050 [5]-[6].

PV systems are utilised in both off-grid and grid-connected applications [7]. Grid-connected PV systems are tied to the distribution network through the power electronics converters. It is well-known that cascade connection of DC-DC boost converters with DC-AC inverters are used widely in grid tied PV systems. DC-DC converters are employed to boost the output voltage of PV panels up to the grid peak voltage levels. This will enable the elimination of coupling step up bulky transformers. Also, maximum power point tracking (MPPT) of the PV sources can be implemented within the closed-loop controller of boost converter. The next converter within the structure of

conventional PV systems is DC to AC inverter which is responsible for conversion of the PV DC output power to AC power, reactive power support of the local loads [8], and active power filtering [9]. It should be noted that both features of the grid-connected PV systems - MPPT and DC to AC conversion – can be implemented in a DC to AC inverter with the help of DC-DC converter, if boost chopper is removed from the structure of the grid connected PV systems. In this situation, MPPT of the PV will be performed through the DC link control loop which should be considered in the closed loop controller of the inverter. However, since the output voltage of photovoltaic systems is far less than the grid voltage level, the PV voltage should be increased significantly in the transformer less PV system. Although output voltage level of PV sources can be increased directly by series connection of the PV panels, this is not a promising approach due to some technical issue e.g. partial shading [10]. Hence for amplification of the PV output voltage, the applications of DC-DC boost converters between PV panels and DC-AC inverter is mandatory [11].

The major criteria for selection of DC-DC converters in PV applications are power density, power efficiency, and number of needed components. For this reason, very high-gain DC-DC converters aren't employed widely in the practical and industrial applications due to higher cost and lower efficient than standard DC-DC converters. Among the standard DC-DC converters e.g. boost, buck, Cuk, SEPIC and buck-boost converters, the standard boost DC-DC converter is used more widely in PV applications due to non-pulsating input current waveform and simpler structure [12].

From controller design viewpoint, closed-loop control of the DC-DC boost converter is a challenging task due to non-minimum phase characteristics of the boost converters. To cope with this issue, the application of the cascaded controllers is reported for stabilization of the DC-DC boost converted using a different range of modern controllers e.g. PI-Back Stepping, PI-Adaptive, PI-

Fuzzy [13] and Fuzzy-Back Stepping [14]. The main idea behind the cascade control of the boost converter is indirect regulation of the output voltage through current control of the converter's inductor. Two different loops which e.g. outer and inner loops, are employed indeed for output voltage and inductor current control respectively. Actually, a current controller determines the converter's duty cycle in an inner loop while its reference value is determined using the output voltage error [15]

Also, application of the DC-AC inverter is mandatory in grid-connected PV systems. Considering the voltage level of PV source, inverters can be implemented either as a single-stage converter or as a two-stage system. In single-stage systems, PV panels are directly connected to the inverter DC link. Despite the simplicity of structure, implementation of MPPT is a bit challenging task in this approach. Actually, a single controller should be designed for both MPPT and AC power control of the DC-AC inverter. Hence, controller design for a single-stage inverter can be assumed as a single-input multi-output (SIMO) problem.

In two-stage PV systems, the PV panels are connected to the inverter's DC link through a DC-DC boost converter. In this approach, the MPPT of PV source is accomplished through the closed-loop control of DC-DC converter. Also, closed-loop controller of the inverter is responsible for AC side power control and DC link voltage regulation. Also, the controller of inverter determines the power quality of the supplied energy. It is well-known that malfunctioning of inverter closed-loop controller might lead to resonance issues at the point of common coupling in a wide range of operation [16]. Hence, the control strategy of the grid-connected inverter has a huge impact on the performance of the photovoltaic system. Application of single-phase H-bridge DC-AC inverter has been widely reported in grid connected PV systems due to simplicity of implementation and modulation techniques and lower voltage stress across the

switches. Also, it enjoys lower-power loss than multi-level and complicated structures.

In reference [17], to maintain the power balance between the injected AC power and the output power of the inverter, a direct controller is employed for output voltage vector control of the inverter which enjoys a simpler implementation. However in this approach, the measurement delays reversely impact on the exchanged power and can lead to a significant error between the desired and real values. Hence, the direct control of the output voltage of inverter is not very promising approach for closed loop control of the grid-connected PV systems.

In reference [18], the indirect AC power controller is investigated which controls the exchanged between grid and z-source inverter. Due to fixed characterise of the power grid - which can modelled as an AC voltage source - the power exchange between grid and inverter can be adjusted indirectly by output current control of the inverter. Regarding the practical issues, this control method is more interesting since the measurement delays don't have a direct impact on the amplitude and phase-angle of the grid current vector. For this reason, application of the current controller for indirect power control of the grid connected DGs are widely employed [19]-[20].

In reference [21], a zeta converter is used for grid connection of the renewable energy sources. Two separate closed-loop controllers are used for the dc and ac sides. In this reference, special attention has been paid to the minimum phase problem of the zeta converter. In order to solve this problem, the developed controller has been used to regulate the dc link voltage indirectly. Hence, the dc side controller is able to mitigate the non-minimum phase issues satisfactorily. However, the zeta converter has a pulsating current waveform at the input terminal and hence, large filters are needed for PV current smoothing and implementation of the MPPT controller using a zeta converter.

In reference [22], a grid-connected photovoltaic system has been investigated, which uses the SEPIC dc-dc converter for MPPT tracking. SEPIC converter is one of the practical and widely used boost converters in the photovoltaic applications. In this reference, a linear control method has been used to control the DC and AC side power. The controllers are tuned with the help of the genetic algorithm. It is not necessary to mention that the whole system, DC-DC converter connected to the Dc-AC inverter, is a MIMO system from the control design viewpoint. However, in this reference, the closed loop system has been separated into two isolated SISO subsystems and actually, the subsystems are employed isolated for controller design at both DC and AC sides. Hence, the application of SISO controllers for a MIMO system cannot guarantee the superior performance of the developed controller at different operating points.

In reference [23], two parallel DC-DC boost converters with an input photovoltaic and a fuel cell sources are presented for grid-connected applications. The MIMO linear closed-loop control method is developed using the averaged state-space model of choppers and inverters. However, in the proposed controller, an MPPT of both photovoltaic and fuel cell sources is achieved using a linear controller. The simulation results show that the proposed MIMO linear controller is stable against DC link capacitor voltage ripple. However, this linear controller can only maintain the stability of system only in a small range of load and input voltage changes, because it is designed based on small signal approximation of a nonlinear plant.

Different aspects of the DC-DC boost converters cascaded with a grid-connected inverters have been carried out in the literature and different types of controllers are studied successfully. A variety of modern controllers has been proposed and investigated in order to achieve a stable response of the grid-connected photovoltaic system. If the control reference value changes e.g. due to a sudden change in the environmental conditions, the closed loop controller

must be fast and robust enough to meet the requirements of the closed-loop system and to stabilize the whole system. Various linear control methods have been introduced for power electronics converters, which can maintain stability only in a small operating range of load and input voltage changes [24]. It is well-known that due to the inherent nonlinear nature of power electronic converters, closed-loop control of these systems is a challenging task indeed. Considering the switching phenomena, the state-space average model has a nonlinear characteristic and for this reason, variety of nonlinear control methods e.g. nonlinear backstepping [25], Fuzzy [26], Feedback linearization [27], Sliding mode [28], Adaptive [29], Lyapunov-based [30] and also hybrid-approaches is proposed to either DC-Dc boost converter or DC-AC grid-connected inverter separately. The nonlinear control techniques can make the response more robust and maintain stability in a wide working range.

In [31], a parallel dc-dc step-up converter connected to the DC link of a three-phase inverter is investigated within a microgrid. Also, a non-linear control method based on the feedback linearization approach has been used to control the parallel boost converters. In the feedback linearization method, the idea of converting the nonlinear system model into a new linear system is used. As a result, a linear controllers can be employed for the exactly linearized nonlinear system in this approach. This controller is a model-based method and requires an accurate model of the system, so it is not straightforward to use this type of nonlinear controller directly either when the accurate model of system isn't available or if there are model uncertainties. If another auxiliary control method is combined with the feedback linearization controller, it can be employed more efficiently to cope with the model uncertainties. However, extra hybrid controller will increase the complexity of system. Among the model-based controllers, the sliding mode nonlinear controller provides a more robust control method against uncertainties. From the controller design perspective, to separate

the controller design problem in the cascaded DC-DC and DC-AC converter, some approximations should be assumed to remove the mutual interconnection between DC-DC and DC-AC converters and to simplify the controller design. The required approximation for isolated controller design for DC-DC and DC-AC converter can be summarized as follows:

- 1- Neglecting the loading of DC-AC inverter on the DC-DC chopper
- 2- Neglecting the inverter DC link voltage ripple

Hence, it is clear that separate controller design cannot guarantee the stability and robustness of the system, if these assumptions are not correct in an operating point. So, the significance of a unified integrated controller for both DC-DC and DC-AC converters in the grid connected PV systems can be observed. Actually, for more reliable and accurate controller design, a compact model which describes both DC-DC and DC-AC converters within a unified comprehensive model should be employed. According to our research and try, such a nonlinear controller that employs the comprehensive unified model of grid connected PV systems has not been reported.

In this article, unified comprehensive MIMO SMC is developed for closed-loop control of the grid connected photovoltaic systems. The power topology includes a boost DC-DC in the first stage cascaded with a single phase full bridge inverter in the second stage. The boost chopper is responsible for MPPT of the PV panels and also, it boosts up the voltage level of the PV source to facilitate the implementation of transformer less grid connected system. Also, DC-AC inverter is responsible for AC power control e.g. active power transfer as well as load compensation. In this study, to realise the unified comprehensive design, whole system is modelled using the averaged state space technique. From the controller design viewpoint, the overall structure of the grid connected PV generator is a multi-input multi-output (MIMO) system. The duty-cycle of the DC-DC converter and inverter modulation index are the control inputs and

on the other hand, generated photovoltaic DC power, and exported power to the grid are control outputs. Moreover, the inverter DC link voltage should be stabilized by the closed-loop controller as well. Briefly, a desired closed-loop controller should achieve five control goals simultaneously as follows:

- 1) To guarantee the stability and robustness of the closed-loop control system in a wide range of parameter changes.
- 2) MPPT of the photovoltaic panel
- 3) Closed-loop control and stabilization of the DC link voltage
- 4) dealing with the non-minimum phase characteristic of the DC-DC boost converter.
- 5) Closed-loop control of the AC power in terms of active power injection as well as load compensation

To achieve the mentioned goals, a unified comprehensive MIMO SMC nonlinear controller is proposed to stabilize the closed loop system using the compact state space model. The proposed MIMO nonlinear controller can be employed in a wide range of changes and uncertainties. It has also been shown that the proposed controller is stable and robust against input voltage and load changes. The steady-state and dynamic responses of the proposed control method have been compared with the linear controllers using the in the simulation results. Comparison of the simulation results of the proposed sliding mode control method and a traditional PI linear control in similar situations shows that:

1. The DC link capacitor voltage overshoot at the converter start-up is lower in the proposed method.
2. The proposed controller has a more stable and robust response against input voltage and load changes.

It should be noted that in terms of practical implementation, the proposed sliding mode controller enjoys simpler structure than other nonlinear controllers.

The structure of this paper is as follows. The circuit structure and analysis of its different operating modes are described in section 2. In the third part, the dynamic modelling of the converter and in the 4th part, the control system design and the compensation network are given. Finally, the simulation results of the designed controller are shown in section 5.

2- The Studied System

The structure of the cascaded DC-DC boost converter with the single-phase grid-connected voltage-source-inverter used in the photovoltaic application is shown in Fig.1. According to Fig. 2, it can be seen that d is the duty cycle of the DC-DC converter and u represents the inverter modulation index. Also, according to the bipolar switching of the single-phase inverter, the equivalent circuit model of Fig. 3 can be employed. According to the equivalent circuit of the inverter, it can be concluded that the input current of the single-phase inverter and output voltage are equal to ui_{L_g} and uV_{C_2} respectively where u is the modulation index of the inverter.

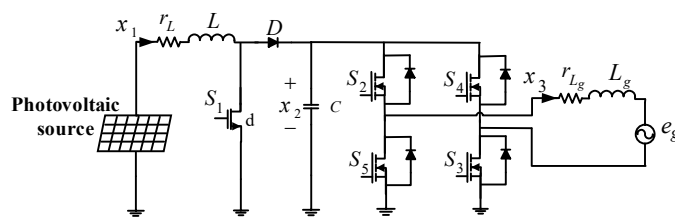


Fig. 1. A DC-DC boost converter cascaded with a single-phase grid-connected H-bridge inverter

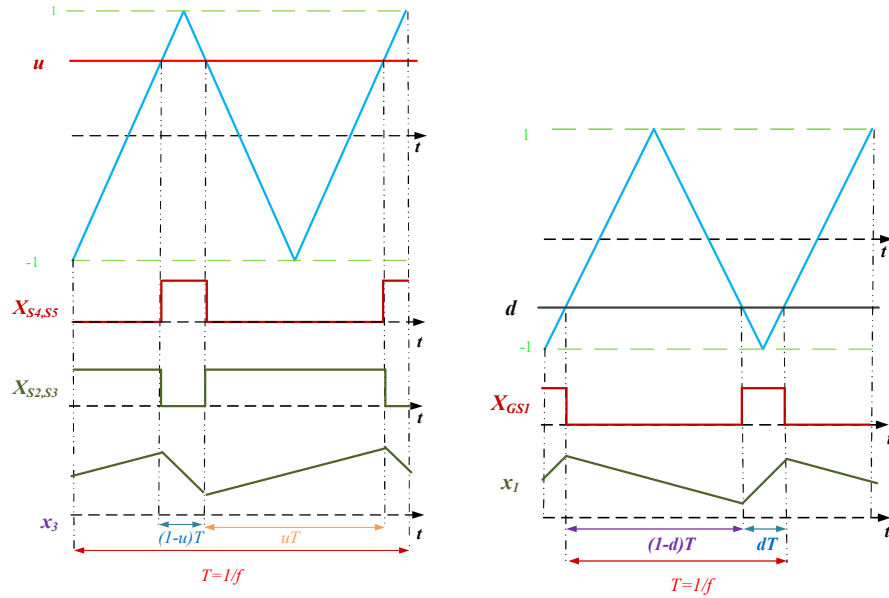


Fig. 2. The critical waveforms of the DC-DC boost converter cascaded with the single-phase grid-connected inverter source to feed the grid

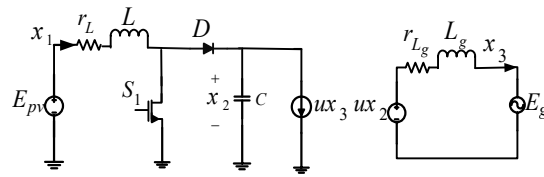
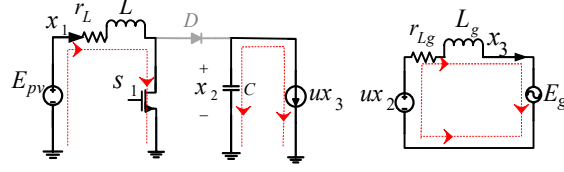
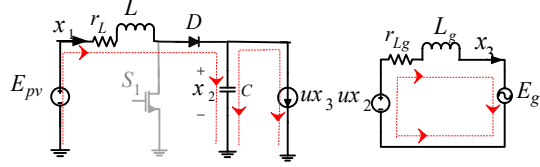


Fig. 3. Equivalent circuit of DC-DC and DC-AC converters

According to Fig. 3, it can be seen that the DC-DC boost converter is fed through a photovoltaic source at the input port. The studied photovoltaic system is a MIMO system from the control point of view. Its control inputs are the duty cycle of the DC-DC converter on the dc side and the amplitude modulation index of the inverter on the ac side. Also, the grid current, PV current and DC link voltage are the control outputs. Considering the parasitic series resistances of the inductors, the equivalent circuit of the studied system is shown in Fig. 4. Considering the different statuses of the switching signal, operating modes of the converter are shown in Fig. 4-a and Fig. 4-b.



a) Equivalent circuit of the converter in the $0 < t < dT$ interval



b) Equivalent circuit of the converter in the $dT < t < T$ interval

Fig. 4. Equivalent circuits and operating modes of the boost DC-DC converter cascaded with the single-phase grid-connected inverter

In Fig. 4, the operation of DC-DC and DC-AC converters are summarised. Within the $0 < t < dT$ range Fig. 4-a, the inductor L is charged through the input PV source. According to Fig. 4-a, and considering the state variables of the circuit and control inputs, the state-space model of the power circuit can be written as follow.

$$\dot{x}_{1,on} = \frac{-r_L}{L} x_1 + \frac{E_{pv}}{L} \quad (1-a)$$

$$\dot{x}_{2,on} = \frac{-u}{C} x_3 \quad (1-b)$$

$$\dot{x}_{3,on} = \frac{u}{L_g} x_2 + \frac{-r_{Lg}}{L_g} x_3 + \frac{-E_g}{L_g} \quad (1-c)$$

Within the next time interval, when $dT < t < T$, the state-space model can be written as follows, considering Fig. 4-b.

$$\dot{x}_{1,off} = \frac{-r_L}{L} x_1 + \frac{-x_2}{L} + \frac{E_{pv}}{L} \quad (2-a)$$

$$\dot{x}_{2,off} = \frac{x_1}{C} - \frac{u}{C} x_3 \quad (2-b)$$

$$\dot{x}_{3,off} = \frac{u}{L_g} x_2 - \frac{r_{Lg}}{L_g} x_3 - \frac{E_g}{L_g} \quad (2-c)$$

By averaging the state-space equations explained in (1-a)-(1-c) over a period e.g. $0 < t < T$, the averaged state-space model of the DC-DC and DC-AC system is obtained as follows:

$$\dot{x}_1 = \left(\frac{E_{pv} - r_L x_1 - x_2}{L} \right) + \left(\frac{x_2}{L} \right) d \quad (3)$$

$$\dot{x}_2 = \left(\frac{x_1}{C} \right) + \left(-\frac{x_1}{C} \right) d + \left(\frac{-x_3}{C} \right) u \quad (4)$$

$$\dot{x}_3 = \left(\frac{-r_{Lg} x_3 - E_g}{L_g} \right) + \left(\frac{x_2}{L_g} \right) u \quad (5)$$

So, the compact and complete dynamic model of the studied system can be rewritten as below, considering the nominal values and uncertainties of the model parameters:

$$\dot{x}_1 = g_1(x_1, x_2, x_3, t) + h_1(x_1, x_2, x_3, t)d = (\hat{g}_1 + \tilde{g}_1) + (\hat{h}_1 + \tilde{h}_1)d \quad (6)$$

$$\dot{x}_2 = g_2(x_1, x_2, x_3) + h_2(x_1, x_2, x_3)d + b_2(x_1, x_2, x_3, t)u = \hat{g}_2 + \tilde{g}_2 + (\hat{h}_2 + \tilde{h}_2)d + (\hat{h}_3 + \tilde{h}_3)u \quad (7)$$

$$\dot{x}_3 = g_3(x_1, x_2, x_3) + b_3(x_1, x_2, x_3)u = \hat{g}_3 + \tilde{g}_3 + (\hat{h}_4 + \tilde{h}_4)u \quad (8)$$

Where in this equation, $\hat{f}_i, \tilde{b}_{iU}$ are nominal values and $i = 1.2.3$, $U = [d \ u]$ are model uncertainties. Also, the control input is defined as d where d is the chopper duty cycle and u is the inverter modulation index. Also, DC link voltage error can be written as:

$$e_{x_2} = x_2^* - x_2 \quad (9)$$

In order to solve the inherent non-minimum phase problem in the direct control of dc link capacitor voltage, the indirect control method has been developed. So, the reference value for a peak of the AC grid current can be written as:

$$x_3^* = (k_p e_{x_2} + k_i \int e_{x_2} dt) \quad (10)$$

$$\dot{x}_3^* = -k_p \left(\frac{x_1}{c} - \frac{x_1}{c} d - \frac{x_3}{c} u \right) + k_i e_{x_2} \quad (11)$$

In this equation, $\sin(\theta)$ is obtained using a phase-locked loop (PLL) based on the grid voltage. The reference signal of controllers are x_1^* and x_2^* . Considering equation (12), the first sliding surface is developed for the DC side of the inverter. In this equation x_1^* is the reference current of the boost DC-DC converter. Also, the sliding surface of ac variables is given by equation (13). It should be noted that x_3^* refers to the reference of inverter output current. Moreover, α_1 is positive and fixed control parameter.

$$S_{1d} = x_1^* - x_1 + \alpha_1 \int (x_1^* - x_1) dt \quad (12)$$

$$S_{2u} = x_3^* - x_3 \quad (13)$$

Control efforts can be calculated by setting the time derivatives of the sliding surfaces to zero.

$$\dot{S}_{1d} = \dot{x}_1^* - \dot{x}_1 + \alpha_1 (x_1^* - x_1) = 0 \quad (14)$$

$$\dot{S}_{2u} = \dot{x}_3^* - \dot{x}_3 = 0 \quad (15)$$

By placing (3) in equation (14), the value of controller d can be rewritten as follows:

$$d = \frac{x_2 - E_{pv} + r_L x_1 + L \alpha_1 (x_1^* - x_1)}{x_2} \quad (16)$$

To obtain the value of u , \dot{x}_3^* should first be calculated from equation (11) at first. By placing equation (16) in equation (11), it can be rewritten as follows:

$$\dot{x}_3^* = \left(-k_p \left(\frac{x_1}{c} - \frac{x_1}{c} \left(\frac{x_2 - E_{pv} + r_L x_1 + L \alpha_1 (x_1^* - x_1)}{x_2} \right) - \frac{x_3}{c} u \right) + k_i (x_2^* - x_2) \right) \quad (17)$$

By making zero equal to \dot{x}_3^* of equation (17) and solving that equation, u is obtained as follows.

$$u = \frac{k_p x_1 L g (-E_{pv} + r_L x_1 + L \alpha_1 (x_1^* - x_1)) + C k_i L g x_2 (x_2^* - x_2) + C x_2 E_g + C x_2 x_3 r_L g}{C x_2^2 - K_p x_2 x_3 L g} \quad (18)$$

The nonlinear model of dc side of system (boost converter and dc-link capacitor) and the ac side (inverter connected to the grid) are written in equations (19)-(21). By averaging over one-half of period, the averaged nonlinear model is obtained from the above relations as follows.

$$\dot{x}_1 = \alpha_1(x_1^* - x_1) \quad (19)$$

$$\dot{x}_2 = \frac{-L_g x_3 k_i (x_2^* - x_2) - x_3 E_g - r_{Lg} x_3^2 + x_1 E_{pv} - r_L x_1^2 - L x_1 \alpha_1 (x_1^* - x_1)}{C x_2 - K_p x_3 L_g} \quad (20)$$

$$\dot{x}_3 = \frac{k_p r_{Lg} \bar{x}_3^2 + k_p x_3 E_g + k_p x_1 L \alpha_1 (x_1^* - x_1) - k_p x_1 E_{pv} + k_p x_1^2 r_L + C x_2 k_i (x_2^* - x_2)}{C x_2 - K_p x_3 L_g} \quad (21)$$

By averaging over one-half of period of AC side, the averaged nonlinear model is obtained from the above relations as follows.

$$\dot{\bar{x}}_1 = \alpha_1(\bar{x}_1^* - \bar{x}_1) \quad (22)$$

$$\dot{\bar{x}}_2 = \frac{-L_g \bar{x}_3 k_i (\bar{x}_2^* - \bar{x}_2) - \frac{\pi^2}{8} \bar{x}_3 E_g - \frac{\pi^2}{8} r_{Lg} \bar{x}_3^2 + \bar{x}_1 E_{pv} - r_L \bar{x}_1^2 - L \bar{x}_1 \alpha_1 (\bar{x}_1^* - \bar{x}_1)}{C \bar{x}_2 - K_p \bar{x}_3 L_g} \quad (23)$$

$$\dot{\bar{x}}_3 = \frac{\frac{\pi^2}{8} k_p r_{Lg} \bar{x}_3^2 + \frac{\pi^2}{8} k_p x_3 E_g + k_p x_1 L \alpha_1 (x_1^* - x_1) - k_p x_1 E_{pv} + k_p x_1^2 r_L + C x_2 k_i (x_2^* - x_2)}{C \bar{x}_2 - K_p \bar{x}_3 L_g} \quad (24)$$

Since it is assumed to be $x_3^* = I_m \sin(\omega t)$, so in half the period of AC side, the average value is $\bar{x}_3^* = \frac{2}{\pi} I_m$.

By equating the derivative of state variables to zero in the equations (22)-(24), operating points for stable performance are obtained as follows.

$$\bar{x}_1 = \bar{x}_1^* \quad (25)$$

$$\bar{x}_2 = \bar{x}_2^* \quad (26)$$

$$\bar{x}_3 = \frac{8 k_p E_{pv} \bar{x}_1^*}{\pi^2 E_g} \quad (27)$$

The Jacobian linearization method around the selected operating point (equations (25)-(27)) has been used in operating small-signal equations (22)-(24) to obtain the control value of nonlinear system.

$$j_{11} = \frac{\partial \dot{\bar{x}}_1}{\partial \bar{x}_1} = -\alpha_1 \quad (28)$$

$$j_{12} = \frac{\partial \dot{\bar{x}}_1}{\partial \bar{x}_2} = j_{13} = 0 \quad (29)$$

$$j_{21} = \frac{\partial \dot{\bar{x}}_2}{\partial \bar{x}_1} = \frac{\pi^2 E_g E_{PV} + \pi^2 E_g L \bar{x}_1^* \alpha_1}{\pi^2 E_g C \bar{x}_2^* - 8k_p L_g E_{PV} \bar{x}_1^*} \quad (30)$$

$$j_{22} = \frac{\partial \dot{\bar{x}}_2}{\partial \bar{x}_2} = \frac{8k_i L_g E_{PV} \bar{x}_1^*}{\pi^2 E_g C \bar{x}_2^* - 8k_p L_g E_{PV} \bar{x}_1^*} \quad (31)$$

$$j_{23} = \frac{\partial \dot{\bar{x}}_2}{\partial \bar{x}_3} = -\frac{\pi^2}{8} E_g \quad (32)$$

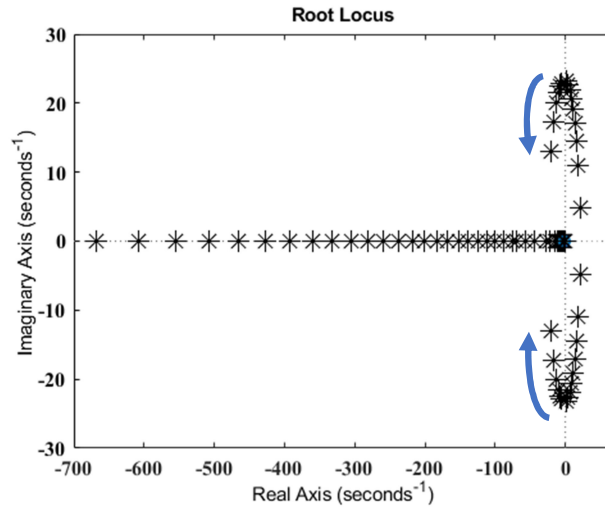
$$j_{31} = \frac{\partial \dot{\bar{x}}_3}{\partial \bar{x}_1} = \frac{-\pi^2 k_p E_g (E_{PV} + L \bar{x}_1^* \alpha_1)}{\pi^2 E_g C \bar{x}_2^* - 8k_p L_g E_{PV} \bar{x}_1^*} \quad (33)$$

$$j_{32} = \frac{\partial \dot{\bar{x}}_3}{\partial \bar{x}_2} = \frac{-\pi^2 k_i C E_g \bar{x}_2^*}{\pi^2 E_g C \bar{x}_2^* - 8k_p L_g E_{PV} \bar{x}_1^*} \quad (34)$$

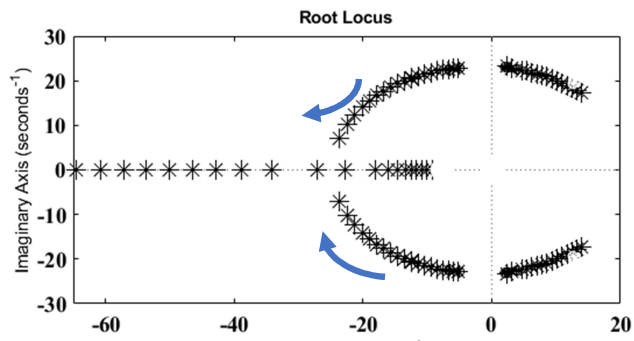
$$j_{33} = \frac{\partial \dot{\bar{x}}_3}{\partial \bar{x}_3} = \frac{\pi^4 E_g k_p}{2\pi^2 E_g C \bar{x}_2^* - 16k_p L_g E_{PV} \bar{x}_1^*} \quad (35)$$

The closed-loop roots of control system are obtained by $G = |SI - J|$. In this regard, there are I unit matrices and J Jacobian matrices by placing the nominal values of parameters. (Table 2 lists the nominal values of parameters). The closed-loop roots of control system are shown in Fig. 3.

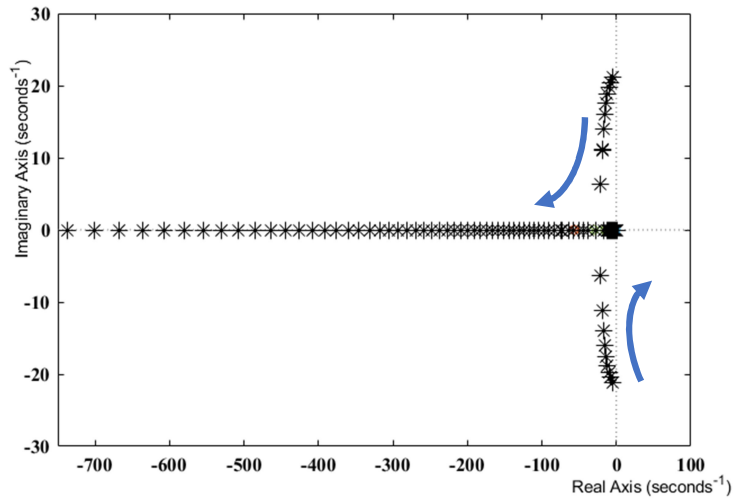
Fig. 5 shows the geometric locations of roots closed-loop control systems in change for a change in control interests α_1 , k_p , k_i .



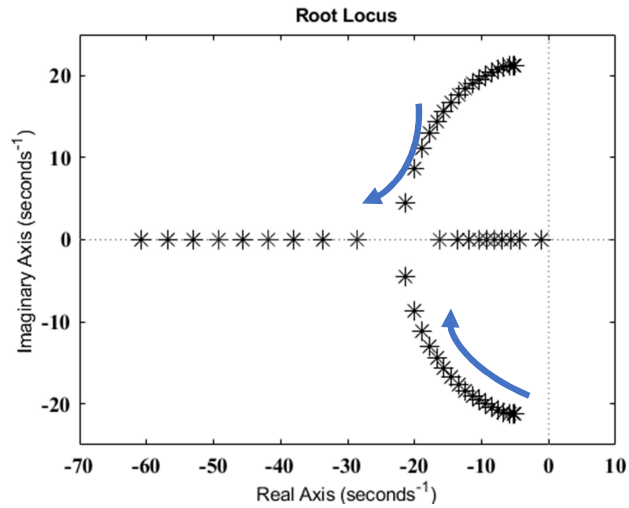
- a) Geometric location of roots ring control system depending on $\alpha_1 = 1$, $k_i = 20$,
 $-5 < k_p < 10$ unstable range.



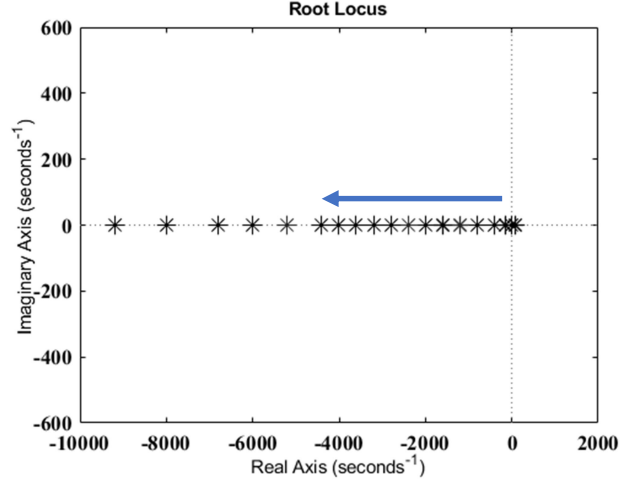
- b) Geometric location of roots ring control system depending on $k_p = 10$, $\alpha_1 = 1$,
 $-10 < k_i < 200$ unstable range



- c) Geometric location of roots ring control system depending on $\alpha_1 = 1, k_i = 20$,
 $1 < k_p < 10$ stable range.



- d) Geometric location of roots ring control system depending on $k_p = 10, \alpha_1 = 1$,
 $0.1 < k_i < 200$ stable range



- e) Geometric location of roots ring control system depending on $k_p = 10$, $k_i = 20$,
 $0.01 < \alpha_1 < 10000$ stable range

Fig 5. Geometric location of closed-loop roots of control system unstable and stable range.

Fig. 5-a and Fig. 5-b shows that for changing the k_p parameter in the range of -5 to 10 and changing the parameter from -10 to 200 geometric locations of roots in the area to the right of jw axis, the system is unstable in this range. But Fig. 5-c, Fig. 5-d, and Fig. 5-e shows the range of changes k_p , k_i and α system stability (the geometric location of roots is on the jw axis).

Since the designed controller has linear and non-linear parts. The system duty cycle can be written as follows.

$$d = \bar{d} + \tilde{d} \quad (36)$$

$$d = \frac{1}{\hat{h}_1} (-\hat{g}_1 + \alpha_1(x_1^* - x_1) - k_1 \text{sgn}(S_{1d})) \quad (37)$$

$$S_{1d} \dot{S}_{1d} = S_{1d} \left(\hat{g}_1 + \frac{h_1}{\hat{h}_1} (-\hat{g}_1 + \alpha_1(x_1^* - x_1) - k_1 \text{sgn}(S_{1d})) \right) \quad (38)$$

$$S_{1d} \dot{S}_{1d} = S_{1d} \left(\hat{g}_1 + \hat{g}_1 \left(1 - \frac{h_1}{\hat{h}_1} \right) + \frac{h_1}{\hat{h}_1} \alpha_1(x_1^* - x_1) - k_1 \frac{h_1}{\hat{h}_1} \text{sgn}(S_{1d}) \right) \quad (39)$$

The stability conditions of control system MIMO-SMC are obtained as follows.

$\frac{-h_1}{\hat{h}_1} \leq -\xi^{-1}$ is a constant control value.

$$S_{1d}\dot{S}_{1d} \leq -\gamma_1 \quad (40)$$

$$S_{1d}\dot{S}_{1d} \leq |S_{1d}||g_1| + |S_{1d}||\hat{g}_1||1 - \xi^{-1}| - k_1\xi^{-1}|S_{1d}| \leq -\gamma_1|S_{1d}| \quad (41)$$

According to the two equations (40) and (41), the value of k_1 is obtained as follows.

$$k_1 \geq \xi(\gamma + g_1) + (\xi - 1)|\hat{g}_1| \quad (42)$$

Since the designed controller has linear and non-linear parts. The system Inverter modulation index can be written as follows.

$$u = \bar{u} + \tilde{u} \quad (43)$$

$$u = \frac{1}{\hat{Q}} \left(-\hat{P} - k_2 \text{sgn}(S_{2u}) \right) \quad (44)$$

Where $\hat{P} = k_p x_1 (E_{pv} - r_L x_1 + L\alpha_1 x_1 - L\alpha_1 x_1^*) - Ck_i(x_2^* - x_2)$ and $\hat{Q} = x_2 x_3$.

$$S_{2u}\dot{S}_{2u} = S_{2u} \left(\hat{P} + \frac{1}{\hat{Q}} \left(-\hat{P} - k_2 \text{sgn}(S_{2u}) \right) \hat{Q} \right) \quad (45)$$

$$S_{2u}\dot{S}_{2u} = S_{2u} \left(g_3 + \hat{P} \left(1 - \frac{Q}{\hat{Q}} \right) - k_2 \frac{Q}{\hat{Q}} \text{sgn}(S_{2u}) \right) \quad (46)$$

The stability conditions of control system MIMO-SMC are obtained as follows.

$\frac{-Q_1}{\hat{Q}_1} \leq -\eta^{-1}$ is a constant control value.

$$S_{2u}\dot{S}_{2u} \leq -\gamma_2 \quad (47)$$

$$S_{2u}\dot{S}_{2u} \leq |S_{2u}||g_3| + |S_{2u}||\hat{P}||1 - \eta^{-1}| - k_2\eta^{-1}|S_{2u}| \leq -\gamma_2|S_{2u}| \quad (48)$$

According to the two equations (47) and (48), the value of k_2 is obtained as follows.

$$k_2 \geq \eta(\gamma_2 + g_3) + (\eta - 1)|\hat{P}| \quad (49)$$

To evaluate the stability of system, the Lyapunov function method ($V = \frac{S_{1d}^2}{2} + \frac{S_{2u}^2}{2}$)

has been used. To establish the stability of system 2,

$$\dot{V} = S_{1d}\dot{S}_{1d} + S_{2u}\dot{S}_{2u} \quad (50)$$

The derivative of smaller Lyapunov function must be equal to zero ($\dot{V} \leq 0$).

$$S_{1d}\dot{S}_{1d} + S_{2u}\dot{S}_{2u} \leq 0 \quad (51)$$

$$S_{1d}\dot{S}_{1d} + S_{2u}\dot{S}_{2u} \leq -\gamma_1|S_{1d}| - \gamma_2|S_{2u}| \quad (52)$$

A photovoltaic system consists of a large number of photovoltaic systems that are connected in series and in parallel to generate voltage and current. The equivalent circuit of a solar cell is shown in the paper [32]. Considering the mathematical model of photovoltaic array and also the characteristic diagram of voltage in terms of current and voltage in terms of power of photovoltaic array to track the maximum power point is shown in Fig. 2 of article [32].

In this study, a new method for modelling and nonlinear closed-loop control based on the sliding mode control method is proposed. In linear controllers, the method of small-signal modelling around a specific point is used, but not paying attention to the nonlinear nature of system leads to the unstable behaviour of system in a relatively wide operating range. As a result, the output is unfavourable and the dc-link capacitor voltage is not stabilized.

Considering the topology of circuit series connection and considering the advantage of not separating the MIMO system into two SISO parts, a unique modelling method has been used for system analysis. The system in question (series amplifier converter with grid-connected VSI inverter) is a MIMO system in terms of control. Therefore, a multi-input multi-output controller is required to fit the control inputs and outputs. The control inputs and outputs on each of proposed MIMO-SMC controllers are designed using the unique SSA-MIMO modelling for the boost chopper connected to the VSI inverter. Therefore, the stability and consistency of system are maintained in a wide functional range.

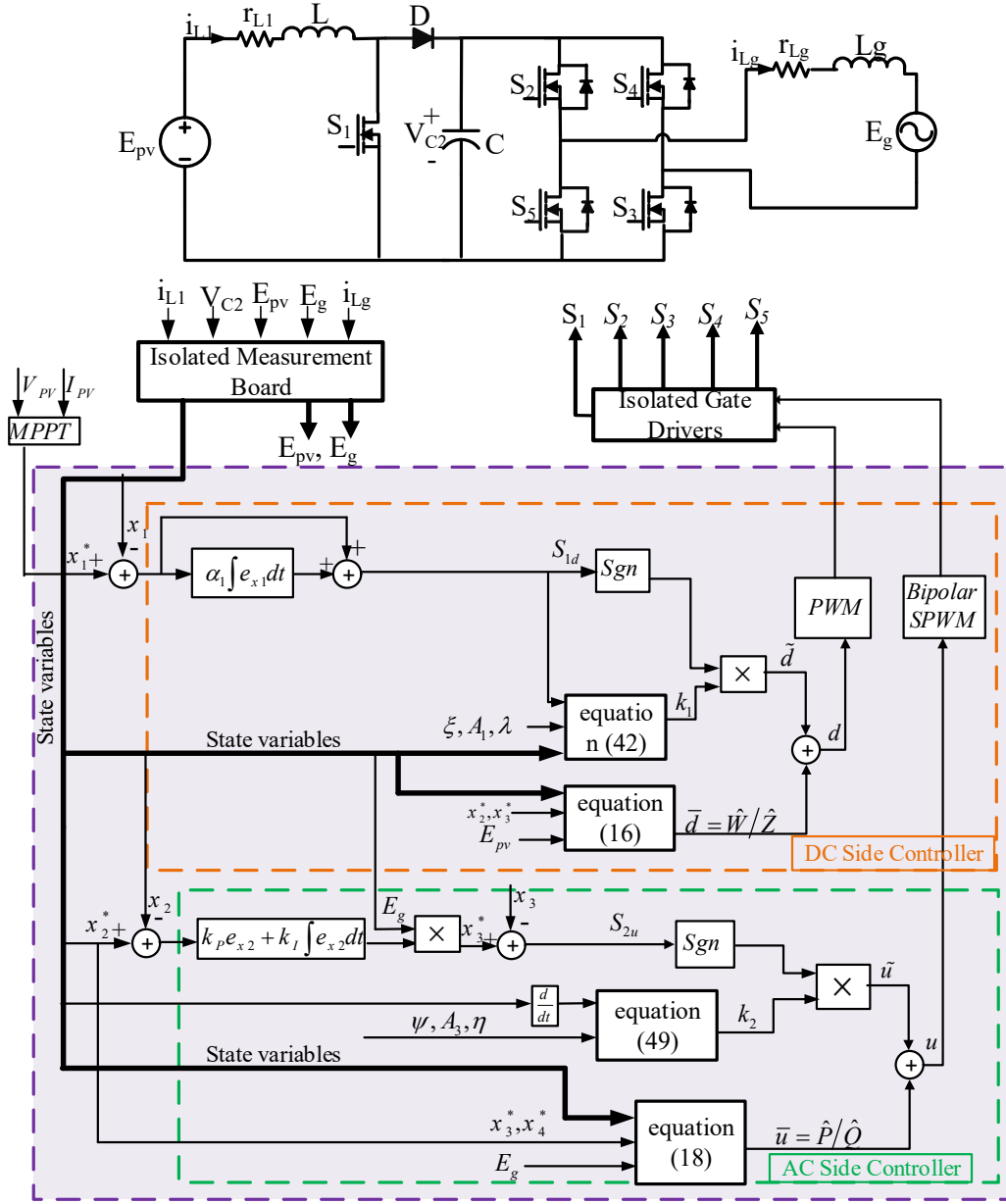


Fig. 6. MIMO system control block diagram

The proposed MIMO-SMC controller block diagram for the grid-connected MIMO system is shown in Fig. 6. Due to the shape of increasing chopper duty cycle and the amplitude modulation index of VSI inverter, the controller input and the current injected into the grid and the current received from the photovoltaic source are the control output of system and all control inputs and outputs and mode variables affect both controllers.

According to Fig. 5, the boost chopper duty cycle is determined in such a way that the maximum power is received from the input source. Considering equation (18), it is adjusted in such a way that the inductor current of boost reaches the relevant reference value and is stabilized in it. It should be noted that the reference value of solar array current (x_1^{ref}) is calculated by the simulation software to achieve the maximum power point function. The reference current of grid must be calculated so that all the power generated by the input source is transferred to the grid. If there is a difference between the output power of input source and the received power of grid, this difference is transferred to the link capacitor voltage and as a result, leads to instability and instability of capacitor voltage, and as a result, the power injected into the grid will be reduced. Therefore, to receive the total output power on the grid side, the dc-link capacitor voltage must be followed and the relevant reference value must be followed and stabilized. Therefore, inside the MIMO-SMC controller, the super-plane method has been used to stabilize the voltage of dc-link capacitor and also to solve the non-minimum phase problem.

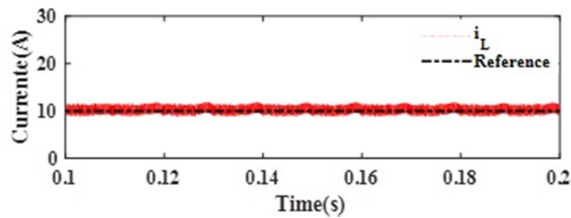
1. Simulation

According to the developed MIMO-SMC control method and in order to evaluate the response of the proposed controller, the simulation results of the converter are presented based on Matlab/Simulink software. It can be seen that the proposed controller can stabilize the boost DC-DC converters cascaded with the grid-connected inverter with zero steady state error. Table (2) shows the nominal parameters of the power circuit.

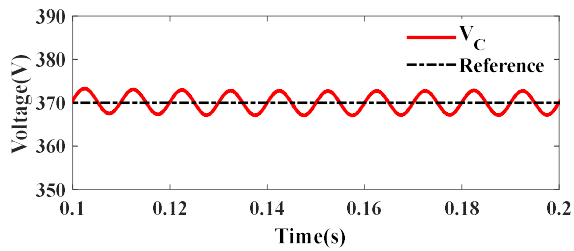
Table 2: nominal parameters of the boost chopper cascaded with a grid connected inverter

<i>Switching frequency</i>	$f_s = 20^{KHz}$
L_1	$L_1 = 1^{mH}$
L_g	$L_g = 1^{mH}$
C	$C = 470^{\mu F}$
<i>Voltage of the PV source</i>	$V_1 = 150^V$
<i>Voltage and frequency of the grid</i>	$V_g = 110^V, f = 50^{Hz}$

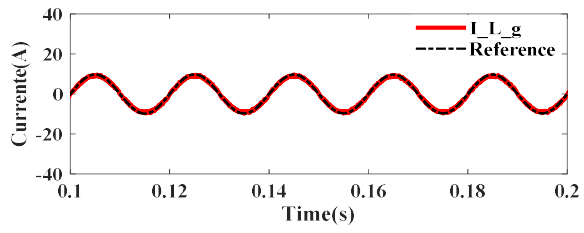
In Fig. 7, the simulation results of the MIMO-SMC controller for the boost DC-DC converters cascaded with the grid-connected inverter are illustrated within the stable operation.



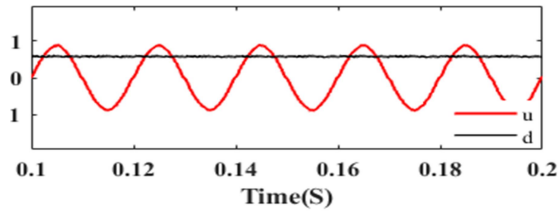
a) PV current



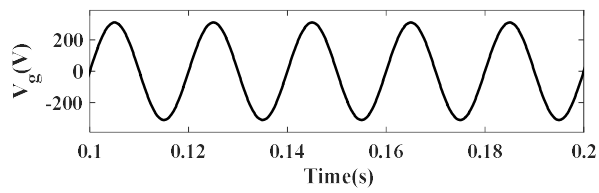
b) DC link voltage



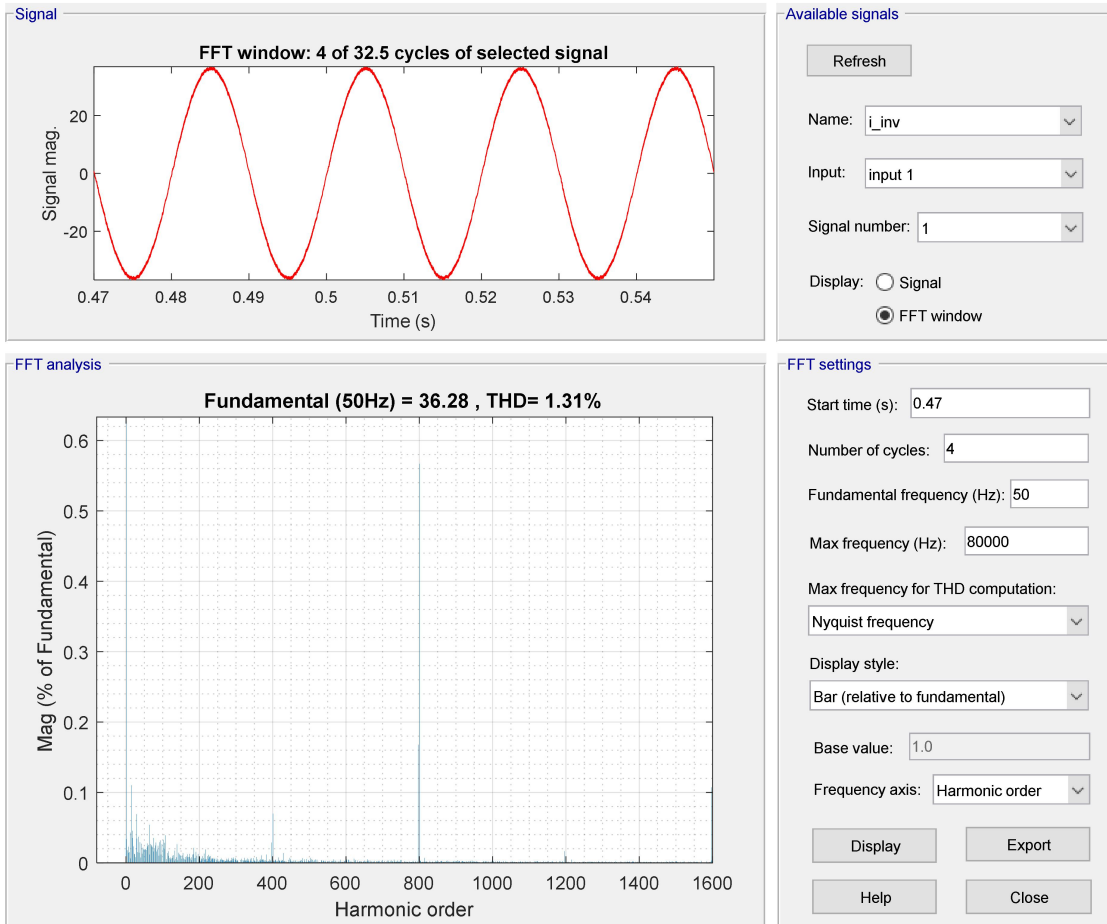
c) grid current



d) duty cycle of the boost DC-DC converter and inverter modulation index



e) grid voltage



f) harmonic spectrum of the grid current

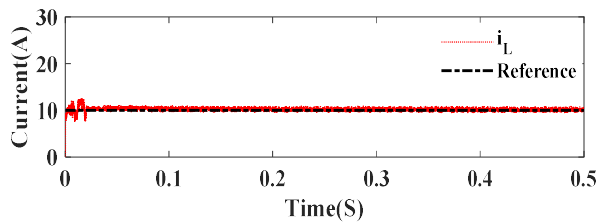
Fig. 7: response of the proposed MIMO sliding mode controller for closed loop control of the DC-DC boost converter cascaded with a single phase grid-connected inverter

The reference current of boost inductor is 10A and the reference voltage of the dc link capacitor is selected as 370V. The grid reference current is calculated using the PI controller based on the DC link voltage error using the hyper plane sliding surface in the proposed controller.

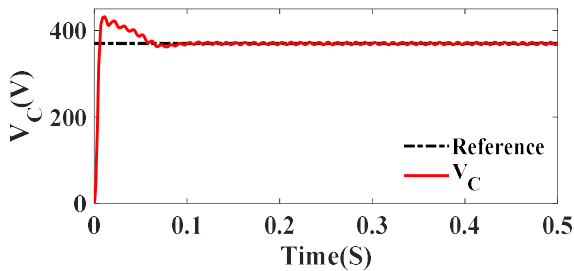
The peak value of the grid reference current is assumed to be 10A. According to Fig. 7-a current PV source follows the reference value appropriately. According to Fig. 7-b, the DC link capacitor voltage follows the reference value appropriately. It is shown that the entire of PV power can be transferred to the grid. Also, the grid reference current is determined using the DC link voltage

error and a PI loop within the hyper-plane sliding model controller. It can be seen in Fig. 7-c that the grid current is equal to the reference value during the steady state operation. The duty cycle and amplitude modulation index of the grid-connected inverter are presented in Fig. 7-d. According to Fig. 7-e, it is clear that the steady state error of the develop controller is zero. Total harmonic distortion is shown in Fig 7-f. According to Fig 7-f, it is clear that when the fundamental (50 Hz) is 36.28, THD equals 1.31%. Also, the THD of the AC current is equal to 1.30%, which complies with the standards of a distribution network.

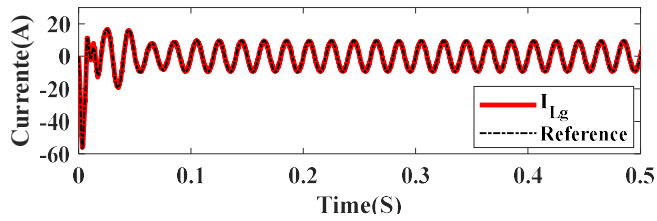
The transient response of the grid-connected photovoltaic system at the start-up is shown in Fig. 8. It shows that the input source current of the changes from zero to the nominal value. It can be seen that the dynamic response of the proposed MIMO-SMC controller is very fast during system at the start point.



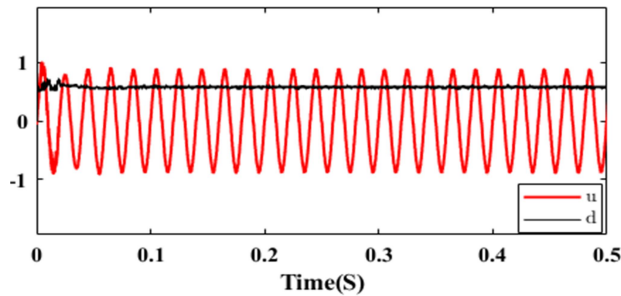
a) PV current



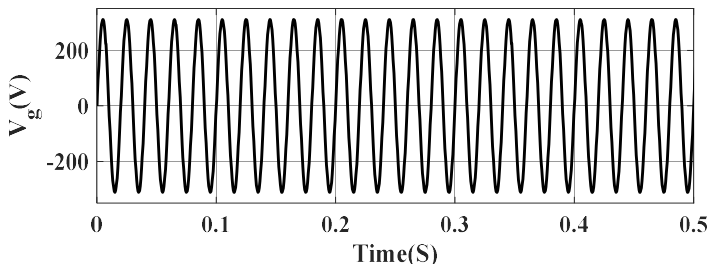
b) DC link voltage



c) grid current



d) duty-cycle and modulation index

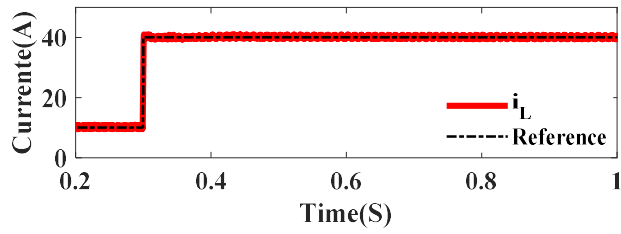


e) grid voltage

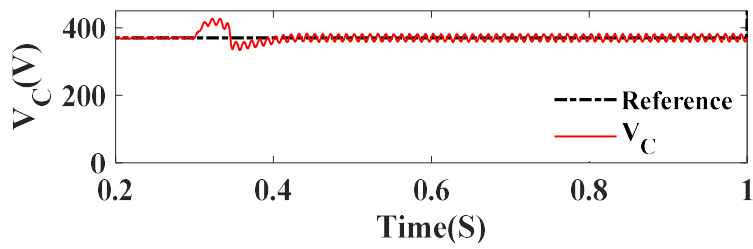
Fig 8. Transient response of the proposed MIMO controller at the start-up

In order to investigate the response of the developed MIMO-SMC controller against input current changes, the simulation results are shown in Fig. 9. It can be seen that the dynamic response of the proposed MIMO-SMC controller is very fast and it is can track the grid reference current with zero steady-state error. Despite large variations in grid current, the proposed MIMO-SMC controller can properly maintain the stability of DC-link voltage within the transients. Also, it can be seen that the boost inductor current (or the output of

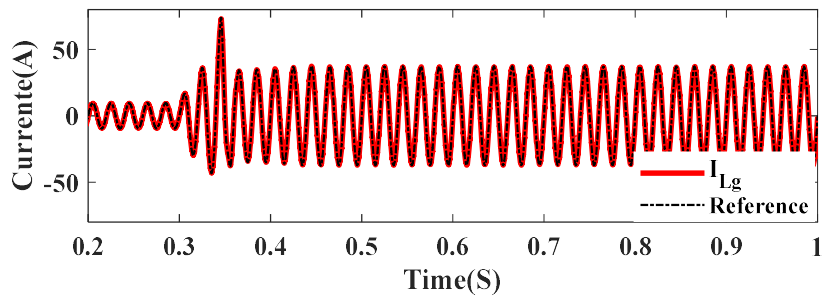
the photovoltaic source) can follow the step changes of the reference signal with zero steady-state error.



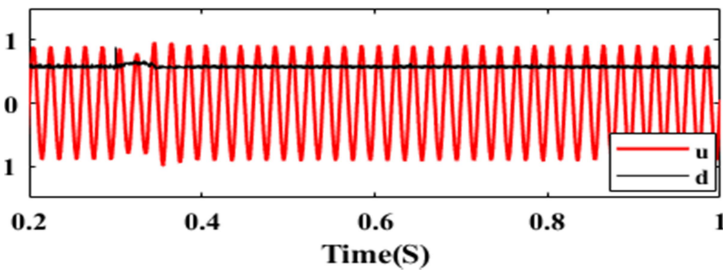
a) PV current



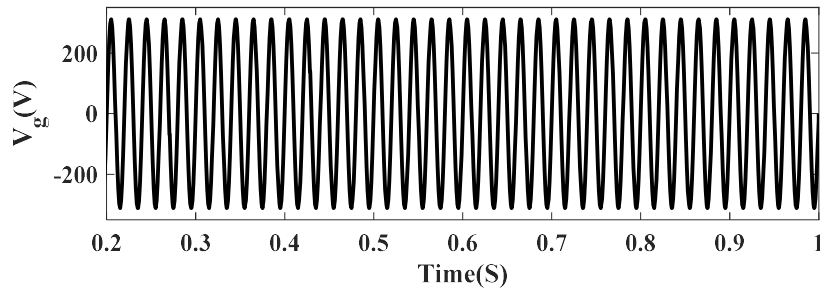
b) dc link capacitor voltage



c) grid current



d) duty cycle and modulation index



e) grid voltage

Fig 9. Dynamic response of the proposed MIMO controller during step changes of the input PV source at $t=0.3s$

It is assumed that the reference value of dc link voltage is increased from 370 to 450 volts at $t=0.3$ s. According to this assumption, the simulation results related to the response of the proposed MIMO-SMC controller as well as response of the conventional PI linear controller to the changes of the DC link voltage reference are shown in Fig. 10. Simulation results show that the proposed controller can track the changes of reference value faster with zero steady state error. Also, the controller has less overshoot at the start-up moment. By comparing the results of the proposed controller and the PI one, the proposed controller is superior overall in term of faster dynamic response and desirable transient characteristics such as overshoot, undershoot.

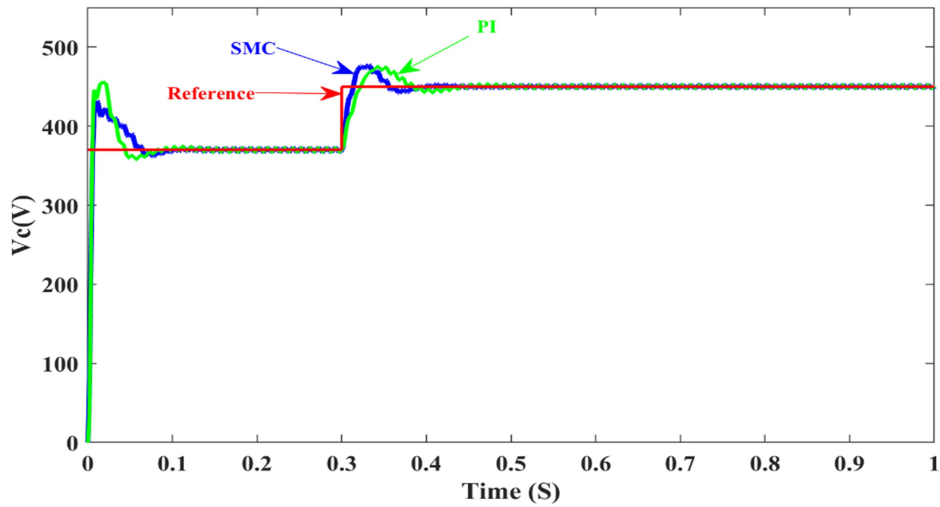


Fig10: DC link voltage changes employed for comparison of the proposed MIMO SMC controller and a PI controller

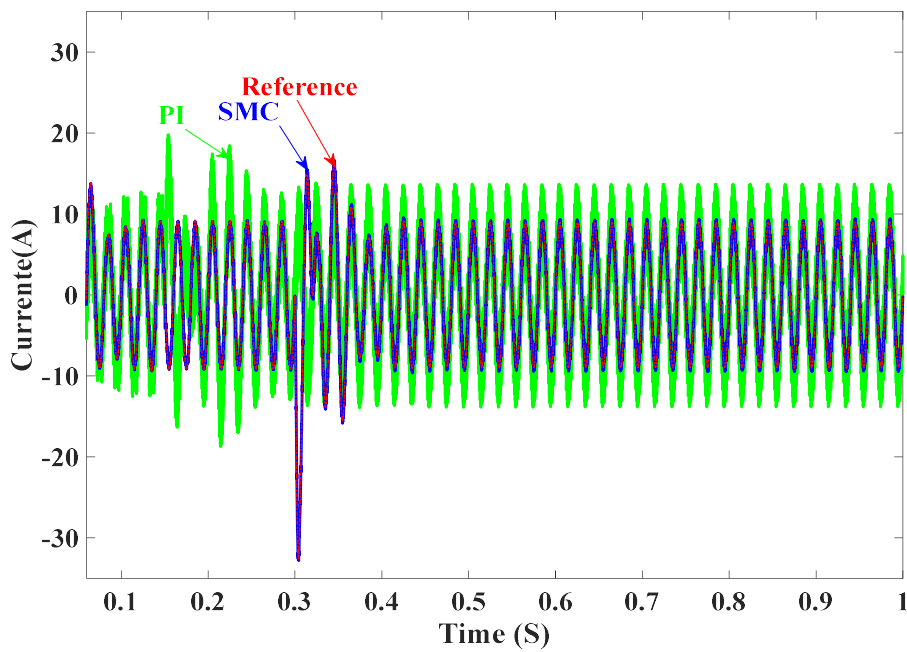


Fig11 :grid voltage and current

The results of simulating the actual amount of injection current into the grid with the two proposed controllers and PI for better comparison are shown in Fig. 11. Fig. 11 shows that the proposed controller follows the reference value of the injected current into the grid well and with high accuracy.

Comparison of the simulation results of the proposed sliding mode control method and linear control of PI under exactly the same conditions shows that:

- 1 The proposed controller has a more resistant response to changes in input voltage and load.
- 2 The voltage of the dc link capacitor at the start-up in the proposed control method is lower than that of the linear control method.
- 3 The proposed controller has a more stable and resistant response due to changes in input voltage and load

2. Conclusion

In this article, a MIMO SMC is developed for a boost DC-DC converter cascaded with the grid connected inverter for PV applications. The duty cycle of the input DC choppers and the modulation index of the inverter are the input variables of the designed multi-input-multi-output controller. The proposed closed loop system is capable of injecting the maximum power of input renewable resources into the grid. For this purpose, the outputs of the control system are defined as currents drawn from input source and grid. Considering the dependence of all converter outputs on each control input, a special compensator network has been used to separate the control loops. Also, by considering the frequency response of the conversion functions of the closed loop system and its optimal phase margin, the parameters of the proposed controller have been set. The obtained results show the effectiveness of the proposed method in a relatively wide working range of network flow changes. Also, the steady state error of the presented control method is zero.

REFERENCES

- [1] K. Sun, K. J. Li, M. Wang, T. Guanyu and Z. Liu. "Coordination control for multi-voltage-level dc grid based on the dc-dc converters" *Electric Power Systems Research.*, vol. 178, no. 1, pp. 106050, Jan 2020.

- [2] J. Ge, C. Shen, K. Zhao, & G. Lv. “Energy production features of rooftop hybrid photovoltaic–wind system and matching analysis with building energy use” *Energy Conversion and Management*, 258, 115485, 2022
- [3] Z. Hekss, A. Abouloifa, I. Lachkar, F. Giri and S. Echalih. “Nonlinear adaptive control design with average performance analysis for photovoltaic system based on half bridge shunt active power filter” *Electric Power & Energy Systems*, vol. 125, no. 1, pp. 106478, Feb 2021
- [4] A. Deshpande, T. Dongare, P. Chaudhari, and S. Borse. “V2G and G2V plug-in and wireless charging integration in Vehicle Parking” *International Research Journal of Engineering and Technology.*, vol. 8, no. 7, 2021.
- [5] E. Ramos, L. Assis, R. Mena, P.Trivino, C.Vazquez and L. Ramirez. “Averaged Dynamic Modeling and Control of a Quasi-Z-Source Inverter for Wind Power Applications” *IEEE Access*, vol. 40, no. 3, pp. 465-473, Jul 2021
- [6] D. Umarani, S. Ramalingam and D. Sambasivan. “Comparative evaluation of PI and fuzzy logic controller for PV grid-tie quasi Z-source multilevel inverter” *Mehran University Research Journal of Engineering & Technology*, vol. 40, no. 3, pp. 465-473, Jul 2021
- [7] S. Kakar, S. Ayob, A. Iqbal, N. Nordin, M. Arif and S. Gore. “New Asymmetrical Modular Multilevel Inverter Topology with Reduced Number of Switches” *IEEE Access*, vol. 9, pp. 27627-27637, February2021
- [8] F. Alizadeh, M. Hosseinpour, A. Dejamkhooy and H. Shayeghi. “Two-Stage Control for Small-Signal Modeling and Power Conditioning of GridConnected Quasi-Z-Source Inverter with LCL Filter for Photovoltaic Generation” *Journal of Operation and Automation in Power Engineering*, vol. 9, no.3 pp. 242-255, Dec 2021.
- [9] L.de Oliveira-Assis, E. P.P Soares-Ramos, R. Sarrias-Mena et al. “Simplified model of battery energy-stored quasi-Z-source inverter-based

- photovoltaic power plant with Twofold energy management system” *Energy* 244: 122563, 2022.
- [10] S. P. Litran, E. Duran, J. Semiao, and R. S. Barroso “Single-Switch Bipolar Output DC-DC Converter for Photovoltaic Application” *Electronics*, vol. 9, no. 7 pp. 1171, 2020
- [11] J. Wang, K. Sun, C. Xue, T. Lio and Y. Li “Multi-Port DC-AC Converter with Differential Power Processing DC-DC Converter and Flexible Power Control for Battery ESS Integrated PV Systems” *IEEE Transactions on Industrial Electronics*, 2021
- [12] W. Dong, S. Li, X. Fu, Z. Li, M. Fairbank and Y. Gao “Control of a Buck dc/dc Converter using Approximate Dynamic Programming and Artificial Neural Networks” *IEEE Transactions on Circuits and Systems*, vol. 68, no. 4, pp. 1760-1768, 2021
- [13] E. Erokhina, M. Kiselev, K. Kryukov, Y. Tserkovsky and M. Lapanov “Analysis of Processes in the Boost DC-DC Converter with Sliding Mode Control” *International Youth Conference on Radio Electronics, Electrical and Power Engineering*, pp. 1-6, 2021
- [14] M. Sellali1, A. Betka1, S. Drid, A. Djerdir et al. “Novel Control Implementation for Electric Vehicles Based on Fuzzy-Back Stepping Approach” *Energy*, 2019.
- [15] T. Ramki, L. N. Tripathy, “Comparison of Different DC-DC Converter for MPPT Application of Photovoltaic System” *International Conference on Electrical, Electronics, Signals, Communication and Optimization*, pp. 1-6, 2015
- [16] H. Mollae, S. M. Ghamari, S. A. Saadat and P. Wheeler. " A novel adaptive cascade controller design on a buck–boost DC–DC converter with a fractional-order PID voltage controller and a self-tuning regulator adaptive current controller," *IET Power Electronics*, vol. 14, no. 11, pp. 312-317, 2021

- [17] M.T. Bina, D.C. Hamill, "Average circuit model for anglecontrolled STATCOM," *IEE Proceedings-Electric Power Applications.*, vol. 152, no. 3, pp. 653-659, 2005.
- [18] A. Zakipour, S. Shokri Kojori, M. Tavakoli Bina, "Closed-loop control of the grid-connected Z-source inverter using hyper-plane MIMO sliding mode," *IET Power Electron.*, vol. 10, PP 2229 – 2241, 2017.
- [19] A. Zakipour, S. Shokri-Kojori, M. Tavakoli Bina, "Sliding mode control of the nonminimum phase grid-connected Z-source inverter" *International Transactions on Electrical Energy Systems.*, vol. 27, no. 11, pp.1-15, 2017.
- [20] N. Ghaffari, A. Zakipour, M. Salimi "State Space Modeling and Sliding Mode Current Control of the Grid Connected Multi-Level Flying Capacitor Inverters" *Journal of Electrical and Computer Engineering Innovations.*, vol. 9, no. 2, pp.215-228, 2021.
- [21] M. Ebadpour, F. Radmand, " Hyper-Plane Sliding Mode Control of Non-Minimum Phase Grid-Connected Zeta Converter," *Power Electronics, Drive Systems, and Technologies Conference.*, pp 1– 5, 2021
- [22] S.Ravikumar, S.Venkatanarayanan. "Gwo Based Controlling of Sepic Converter In Pv Fed Grid Connected Single Phase System" *Microprocessors and Microsystems.*, 2020
- [23] M. Salimi, F. Radmand and M. Hosseini Firrouz. "Dynamic Modeling and Closed-loop Control of Hybrid Grid-connected Renewable Energy System with Multi-input Multi-output Controller" *Journal of Modern Power Systems and Clean Energy.*, vol. 9, no. 1, pp.94-103, 2021.
- [24] S. Roy, P. K. Sahu, S. Jena, A.K. Acharya, "Modeling and control of DC/AC converters for photovoltaic grid-tie micro-inverter application" *Materials Today: Proceedings.*, vol. 39, pp.2027-2036, 2021.
- [25] O. Diouri, N. E. Sbai, F. Errahimi, A. Gaga and C. Alaoui, "Modeling and Design of Single-Phase PV Inverter with MPPT Algorithm Applied to the

- Boost Converter Using Back-Stepping Control in Standalone Mode” *International Journal of Photoenergy.*, no. 6, 2019.
- [26] M. Shadoul, H. Yousef, R. A. Abri and A. Al-Hinai, “Adaptive Fuzzy Approximation Control of PV Grid-Connected Inverters” *Energies.*, vol. 14, no. 4, 2021
- [27] O. Diouri, N. E. Sbai, F. Errahimi, A. Gaga and C. Alaoui, “Voltage control and load sharing in a DC islanded microgrid based on disturbance observer” *Iranian Conference on Electrical Engineering.*, pp. 825-830, 2019.
- [28] S. Roy, P. K. Sahu, S. Jena, A.K. Acharya, “Modeling and control of DC/AC converters for photovoltaic grid-tie micro-inverter application” *Materials Today: Proceedings.*, vol. 39, pp.2027-2036, 2021.
- [29] N. Mahdian, M. Nmvar, H. Karimi, P. piya and M. Karimi-Ghartemani, “Nonlinear adaptive control of grid-connected three-phase inverters for renewable energy applications” *International Journal of Control*, vol. 90, no. 1, pp.53-67, 2017
- [30] A. Abedi, B. Rezaie, A. Khosravi and M. Shahabi, “DC-bus Voltage Control based on Direct Lyapunov Method for a Converterbased Standalone DC Micro-grid” *Electric Power Systems Research.*, no. 6, pp. 106451 2020.
- [31] D. Xu, Y. Dai, C. Yang, & X. Yan, “Adaptive fuzzy sliding mode command-filtered backstepping control for islanded PV microgrid with energy storage system” *Journal of the Franklin Institute.*, vol. 356, no. 4, pp.1880-1898, 2019.
- [32] N. Mohan, T. M. Undeland, and W. P. Robbins, *Power Electronics: Converters, Applications and Design*. New York: John Wiley & Sons Press, 1995.